Synthesis, characterization and opto-electrical properties of ternary Zn_2SnO_4 nanowires

2010 Nanotechnology 21 465706

(http://iopscience.iop.org/0957-4484/21/46/465706)

Nanotechnology **21** (2010) 465706 (4pp) doi:10.1088/0957-4484/21/46/465706

Synthesis, characterization and opto-electrical properties of ternary Zn_2SnO_4 nanowires

Christina Pang[1], Bin Yan, Lei Liao[2], Bo Liu, Zhe Zheng, Tom Wu, Handong Sun and Ting Yu[3]

Division of Physics and Applied Physics, School of Physical and Mathematical Sciences, Nanyang Technological University, 637371, Singapore

E-mail: yuting@ntu.edu.sg

Received 8 September 2010, in final form 4 October 2010
Published 26 October 2010
Online at stacks.iop.org/Nano/21/465706

Abstract

Ternary oxides have the potential to display better electrical and optical properties than the commonly fabricated binary oxides. In our experiments, Zn_2SnO_4 (ZTO) nanowires were synthesized via thermal evaporation and vapor phase transport. The opto-electrical performance of the nanowires was investigated. An individual ZTO nanowire field-effect transistor was successfully fabricated for the first time and shows an on–off ratio of 10^4 and transconductance of 20.6 nS, which demonstrates the promising electronic performance of ZTO nanowire in an electrical device. Field emission experiments on ZTO nanowire film also indicate their potential application as a field emission electron source.

(Some figures in this article are in colour only in the electronic version)

1. Introduction

One-dimensional (1D) metal oxide nanostructures have attracted immense interest due to their unique optical and electrical properties as well as their promising applications in the fabrication of nanodevices [1, 2]. To date, binary oxides have been extensively fabricated and investigated, for example ZnO [3] and CuO [4]. However, there are still few studies involving ternary oxides, which potentially have better properties than binary oxides, some of which include electronic and gas sensing properties [5, 6]. A key advantage of ternary oxides over binary oxides is that properties, such as the electronic structure [7] and thermodynamic properties [8], can be efficiently tuned by varying the proportion of each component [9]. An important ternary oxide, Zn_2SnO_4 (ZTO), has been reported to have high electron mobility, high electrical conductivity and low visible absorption [10, 11], deeming it suitable for applications in thin-film photovoltaic devices, solar cells, and sensors for combustible gases and humidity detection [12, 13].

Previous studies on ZTO nanowires (NWs) have mainly focused on the synthesis [14], growth mechanism [15, 16] and photoluminescence properties [14, 15], with many other physical properties left unexplored. In this paper, ZTO NWs were fabricated and the optical and electrical properties of these ternary oxide NWs were investigated. Individual ZTO NW field-effect transistors (FETs) were configured and their current–voltage (I–V) characteristics with gating were determined. Also, field emission tests of ZTO NWs film were performed.

2. Experimental procedure

Growth of ZTO NWs was conducted in a horizontal tube furnace via thermal evaporation and vapor phase transport. The schematic experimental setup is shown in figure 1. A clean (111)-oriented silicon substrate was first coated with approximately 5 nm Au catalyst film. 0.1 g of ZnO:SnO:C powder mixture with a weight ratio of 1:5:8 was loaded into a small quartz tube of length 30 cm and inner diameter 1.4 cm, with the substrate placed 2 cm downstream from the source.

[1] Present address: Department of Chemistry, Imperial College London, London SW7 2AZ, UK.

[2] Present address: Department of Chemistry and Biochemistry, University of California, Los Angeles, California 90095, USA.

[3] Author to whom any correspondence should be addressed.

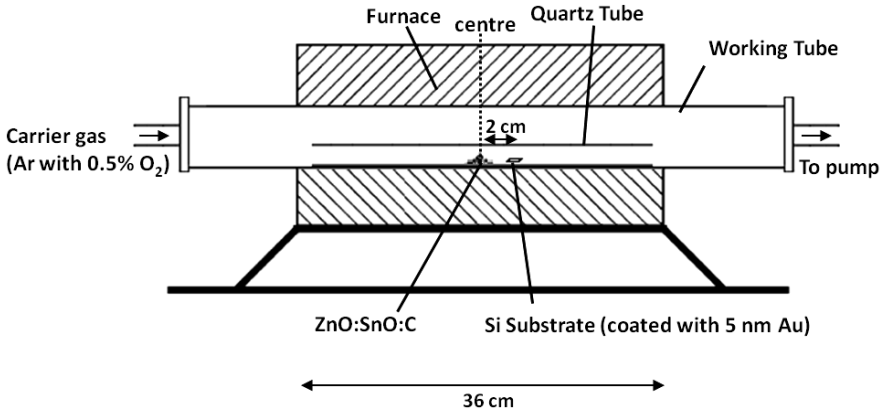

Figure 1. Schematic experimental setup (not drawn to scale) for the growth of ZTO NWs.

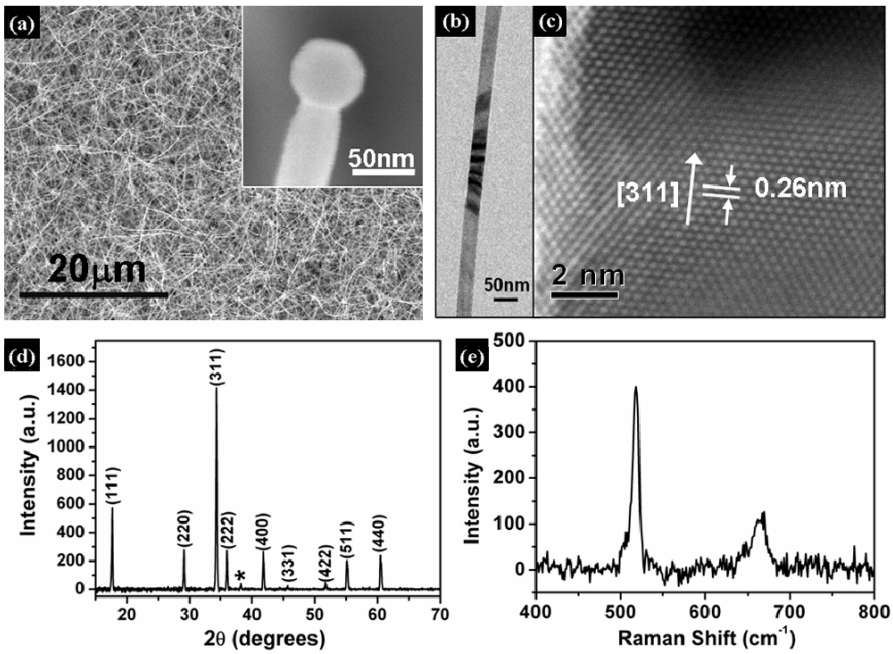

Figure 2. (a) SEM image of ZTO NWs on a Si substrate. Inset shows a high magnification SEM image, showing the presence of a catalyst particle on the tip of the NWs, (b) TEM image of the NW, (c) HR-TEM of side-edge of the NW, (d) XRD pattern of ZTO NWs on a Si substrate, (e) room temperature Raman spectrum of ZTO NWs.

This tube was then inserted into the working tube of length 75 cm and inner diameter 2.2 cm mounted on the furnace, with the source being positioned at the center of the furnace. The furnace was approximately 36 cm in length. The furnace was set to heat to the reaction temperature of 1000 °C and maintained for 1 h. Upon the furnace reaching 750 °C, a constant gas flow (99.5% Ar, 0.5% O_2) at 50 standard cubic centimeters per minute (sccm) was turned on. The gas flow was not turned on at a lower temperature to prevent any undesired formation of ZnO NWs, since the formation of ZnO nanostructures in the presence of graphite requires a lower temperature of approximately 650–700 °C [17]. The purpose of the graphite in precursor mixture was to serve as a reducing agent, so as to obtain Sn and Zn vapor sources.

After being cooled to room temperature, the substrate was characterized using scanning electron microscopy (SEM; JEOL JSM-6700F), x-ray diffraction (XRD; Bruker D-8 Advanced, Cu Kα radiation) and high-resolution transmission electron microscopy (HR-TEM; JEOL JEM-2010F). Raman scattering was measured at room temperature (Witec CRM200, 532 nm excitation). The room temperature photoluminescence (PL) spectrum was also recorded in the spectral range of 420–870 nm using a He–Cd laser with a wavelength of 325 nm as the excitation source.

To prepare the individual NW FET for electrical performance testing, ZTO NWs were removed in ethanol, after which the solution was ultrasonically dispersed and dropped onto SiO_2/Si (i.e. 200 nm insulated SiO_2 film over Si substrate). Subsequently, Au contact pads of 100 nm thickness were fabricated by photolithography and rf-sputtering. The transport properties were measured by a Suss probe station with a Keithley 4200 semiconductor characterization system (SCS).

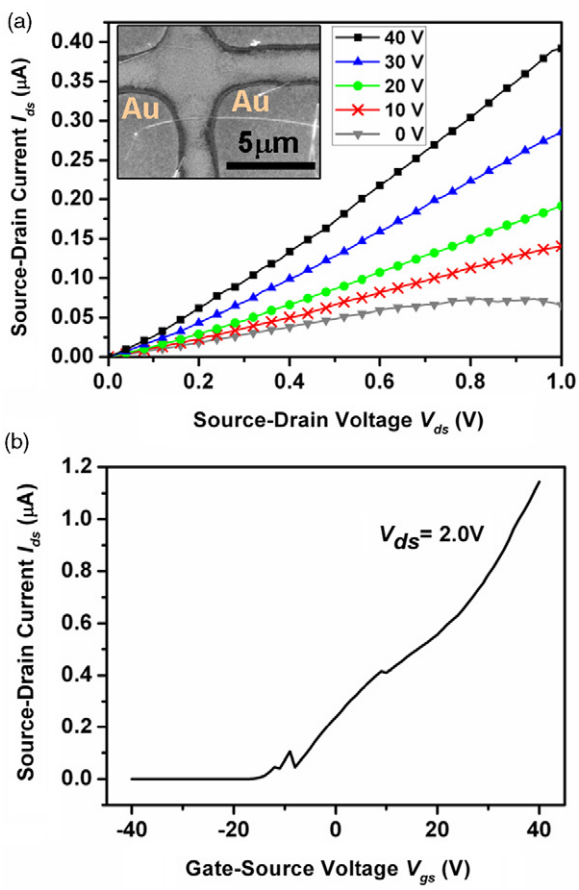

Figure 3. (a) Room temperature I_{ds}–V_{ds} curves at different gate voltages. Inset shows the SEM image of a ZTO NW FET, (b) I_{ds}–V_{gs} curve obtained at $V_{ds} = 2.0$ V.

3. Results and discussion

A typical SEM image is shown in figure 2(a). The NWs are estimated to be about 20 μm in length and between 30 and 50 nm in diameter. Most of the NWs have a smooth outer surface and catalyst particles present on their tips, one of which is seen in the inset of the figure. When the experiment was repeated without the Au coating on substrate, there was almost no NW growth apart from those found at defect sites, which suggests that the growth was dominated by the vapor–liquid–solid (VLS) mechanism [18]. Figure 2(b) shows a typical TEM image of the ZTO NW. The clear lattice fringes in figure 2(c) of the HR-TEM image show the single crystalline nature of the NW. The growth direction, with lattice spacing of 0.26 nm, can be indexed to [311].

Figure 2(d) shows an XRD pattern of the as-grown sample, with almost all the diffraction peaks being indexed to face-centered spinel-structured ZTO, consistent with the standard data file (JCPDS file No. 24-1470). The residual peak marked with an asterisk can be indexed to Au(111) (JCPDS file No. 04-0784), which originates from the catalyst. The absence of any ZnO peaks in our sample shows its high purity. A room temperature Raman spectrum of the NWs is illustrated in the inset of figure 2(e). The Raman peak at 520 cm^{-1} corresponds to Si while that at 666 cm^{-1} corresponds quite well to the well-known ZTO peak [11].

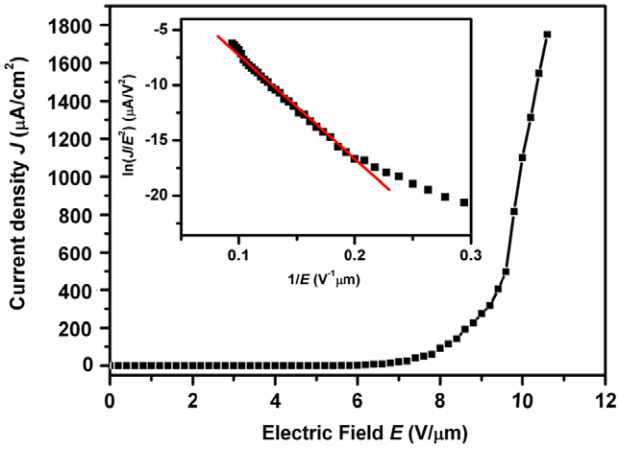

Figure 4. Current density–electric field (J–E) plot of ZTO NWs. Inset shows the Fowler–Nordheim (FN) plot of ZTO NWs with linear dependence (solid line is the fitting result).

The inset of figure 3(a) is a SEM image of a ZTO NW FET showing the channel length between electrodes to be about 3 μm. Figure 3(a) displays the current versus source–drain bias (I_{ds}–V_{ds}) curves obtained under gate–source voltages (V_{gs}) of 0, 10, 20, 30 and 40 V. It is obvious that the conductance of the NW increases monotonically as the gate potential increases, providing evidence that the ZTO NW FET is an n-channel device.

The I_{ds}–V_{gs} curve of a single NW FET is shown in figure 3(b). The on–off ratio at 2.0 V bias (comparing $V_{gs} = -20$ and 20 V) exceeds 10^4. The transconductance (g_m), electron mobility (μ) and capacitance (C) in a typical cylindrical NW with radius r can be expressed as [19]

$$\text{Transconductance } g_m = \frac{dI}{dV_{gs}} \tag{1}$$

$$\text{Electron mobility } \mu = g_m \times \frac{\ln(2h/r)}{2\pi\varepsilon_0\varepsilon} \times \frac{L}{V_{ds}} \tag{2}$$

$$\text{Capacitance } C = \frac{2\pi\varepsilon_0\varepsilon L}{\ln(2h/r)} \tag{3}$$

where h is the gate oxide layer thickness, r is the NW radius, ε is the relative dielectric constant for $SiO_2 = 3.9$ and L is the NW channel length. For $V_{gs} = 2.0$ V, the transconductance $g_m = dI/dV_{gs} = 20.6$ nS can be estimated from the linear region (−8–8 V) of the I_{ds}–V_{gs} curve. The capacitance of the ZTO NW is $C = 2.18 \times 10^{-4}$ pF and the electron mobility was calculated to be $\mu = 4.27$ cm^2 V^{-1} s^{-1} at $V_{gs} = 0$ V. Compared to a ZnO NW FET with similar dimensions [20], our ZTO NW FET displays an enhanced on–off ratio and electron mobility. The good on–off ratio and transconductance of ZTO show the promising electronic performance of this ternary oxide in a FET device.

Field emission studies were conducted on the ZTO NWs using a two parallel-plate setup with an electrode distance of 100 μm, under a vacuum pressure of about 2×10^{-6} Torr. Figure 4 depicts the plot of the typical current density–electric field (J–E) curve, which shows the turn-on field of the NWs to be about 4.7 V μm^{-1} at a current density of 0.2 μA cm^{-2}.

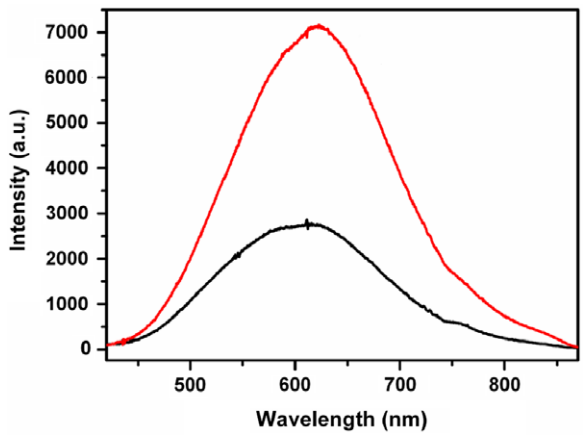

Figure 5. Room temperature PL spectra of ZTO NWs before (red line) and after (black line) annealing in air at 700 °C for 2 h.

The maximum current density attained, which was calculated to be about 1750 μA cm^{-2}, corresponding to electric field of 10.6 V μm^{-1}, can provide enough emission current as a field emitter. The simplified Fowler–Nordheim (FN) equation is given by

$$J = \frac{A\beta^2 E^2}{\Phi} \exp\left[-\frac{B\Phi^{3/2}}{\beta E}\right] \quad (4)$$

where J is the current density, E is the applied field strength, Φ is the work function of ZTO NW, which is estimated to be about 4.9 eV [21], A and B are constants with values 1.54×10^{-6} A V^{-2} eV and 6.83×10^3 V μm^{-1} eV$^{-3/2}$ respectively [22].

The linear $\ln(J/E^2)$ versus $1/E$ plot at high electric fields, shown in the inset of figure 4, suggests that the classical FN mechanism is responsible for the emission from the NWs. β, the field enhancement factor, defined as the ratio of the local electric field, E_{local}, to the average electric field, E (in V μm^{-1}), was found to be 788. This value turned out to be comparable to that of SnO_2 [23] and CuO [4] and is adequate for application as a field emission electron source, though not as high as carbon nanotubes [24]. Improvements in the field emission properties of the NWs can be made through better alignment and density control, by modifying the experimental parameters such as pressure, mass flow etc.

PL spectra of ZTO NWs before and after annealing at 700 °C in air for 2 h are shown in figure 5. In both plots, a stable broad orange peak centered at 610 nm was obtained. After annealing the as-grown ZTO NWs in air for 2 h, the PL peak intensity significantly reduced. The reduction in PL peak intensity after annealing may be attributed to the filling of oxygen vacancies, which results in lower concentrations of oxygen vacancies. In our experiment, the thermal evaporation method was employed to fabricate the NWs, and thus as anticipated, will result in the formation of oxygen vacancies due to insufficient oxygen during the growth process [14]. These oxygen vacancies will induce defect levels within the band gap that generate the orange emission of the ZTO NWs. The annealing effect observed in our experiment can account for the presence of these oxygen vacancies. This mechanism is also consistent with that for ZnO, whose n-type conductivity has been typically attributed to oxygen vacancies [25].

4. Conclusion

In summary, ZTO NWs were synthesized via thermal evaporation and vapor phase transport process. Electrical transport studies were conducted on the fabricated ZTO NW FETs. The on–off ratio and transconductance are estimated to be $\sim 10^4$ and 20.6 nS respectively. Field emission experiments determined the maximum current density to be 1750 μA cm^{-2} and the field enhancement factor as 788. Our experimental results show the great potential ZTO NWs have for applications in nanoscale electronic devices.

Acknowledgment

The authors would like to thank Dr Zhang Jixuan from the Materials Science and Engineering Department, NUS, for her help in TEM Imaging.

References

[1] Xia Y N, Yang P D, Sun Y G, Wu Y Y, Mayers B, Gates B, Yin Y D, Kim F and Yan Y Q 2003 *Adv. Mater.* **15** 353–89
[2] Yan B, Liao L, You Y M, Xu X J, Zheng Z, Shen Z X, Ma J, Tong L M and Yu T 2009 *Adv. Mater.* **21** 2436–40
[3] Liao L, Lu H B, Shuai M, Li J C, Liu Y L, Liu C, Shen Z X and Yu T 2008 *Nanotechnology* **19** 175501
[4] Zhu Y W, Yu T, Cheong F C, Xu X J, Lim C T, Tan V B C, Thong J T L and Sow C H 2005 *Nanotechnology* **16** 88–92
[5] Fan H J, Yang Y and Zacharias M 2009 *J. Mater. Chem.* **19** 885–900
[6] Feng P, Zhang J Y, Wan Q and Wang T H 2007 *J. Appl. Phys.* **102** 074309
[7] Mishra K C, Johnson K H and Schmidt P C 1993 *J. Phys. Chem. Solids* **54** 237–42
[8] Jacob K T, Lwin K T and Waseda Y 2002 *Solid State Sci.* **4** 205–15
[9] Zheng Z, Yan B, Zhang J, You Y, Lim C T, Shen Z and Yu T 2008 *Adv. Mater.* **20** 352–6
[10] Stambolova I, Konstantinov K, Kovacheva D, Peshev P and Donchev T 1997 *J. Solid State Chem.* **128** 305–9
[11] Coutts T J, Young D L, Li X, Mulligan W P and Wu X 2000 *J. Vac. Sci. Technol.* A **18** 2646–60
[12] Belliard F, Connor P A and Irvine J T S 2000 *Solid State Ion.* **135** 163–7
[13] Yu J H and Choi G M 2001 *Sensors Actuators* B **72** 141–8
[14] Wang J X *et al* 2004 *J. Cryst. Growth* **267** 177–83
[15] Su Y, Zhu L-a, Xu L, Chen Y, Xiao H, Zhou Q and Feng Y 2007 *Mater. Lett.* **61** 351–4
[16] Jie J S, Wang G Z, Han X H, Fang J P, Yu Q X, Liao Y, Xu B, Wang Q T and Hou J G 2004 *J. Phys. Chem.* B **108** 8249–53
[17] Li M-K, Wang D-Z, Ding Y-W, Guo X-Y, Ding S and Jin H 2007 *Mater. Sci. Eng.* A **452/453** 417–21
[18] Wagner R S and Ellis W C 1964 *Appl. Phys. Lett.* **4** 89–90
[19] Dattoli E N, Wan Q, Guo W, Chen Y, Pan X and Lu W 2007 *Nano Lett.* **7** 2463–9
[20] Heo Y W, Tien L C, Kwon Y, Norton D P, Pearton S J, Kang B S and Ren F 2004 *Appl. Phys. Lett.* **85** 2274–6
[21] Kurz A and Aegerter M A 2008 *Thin Solid Films* **516** 4513–8
[22] Zhu Y W, Yu T, Sow C H, Liu Y J, Wee A T S, Xu X J, Lim C T and Thong J T L 2005 *Appl. Phys. Lett.* **87** 023103
[23] He J H, Yu T H, Hsin C L, Li K M, Chen L J, Chueh Y L, Chou L J and Wang Z L 2006 *Small* **2** 116–20
[24] Baughman R H, Zakhidov A A and de Heer W A 2002 *Science* **297** 787–92
[25] Janotti A and Van de Walle C G 2005 *Appl. Phys. Lett.* **87** 122102